AMERICAN SOCIETY FOR MICROBIOLOGY | mBio®

RESEARCH ARTICLE

Horizontal Gene Transfer of Functional Type VI Killing Genes by Natural Transformation

Jacob Thomas, Samit S. Watve,* William C. Ratcliff, Brian K. Hammer

School of the Biological Sciences, Georgia Institute of Technology, Atlanta, Georgia, USA

ABSTRACT Horizontal gene transfer (HGT) can have profound effects on bacterial evolution by allowing individuals to rapidly acquire adaptive traits that shape their strategies for competition. One strategy for intermicrobial antagonism often used by *Proteobacteria* is the genetically encoded contact-dependent type VI secretion system (T6SS), a weapon used to kill heteroclonal neighbors by direct injection of toxic effectors. Here, we experimentally demonstrate that *Vibrio cholerae* can acquire new T6SS effector genes via horizontal transfer and utilize them to kill neighboring cells. Replacement of one or more parental alleles with novel effectors allows the recombinant strain to dramatically outcompete its parent. Using spatially explicit modeling, we examine how this process could affect the ecology and evolution of surface-attached microbial populations. HGT of T6SS effector-immunity pairs is risky: transformation brings a cell into conflict with its former clone mates but can be adaptive when superior T6SS alleles are acquired. More generally, we find that these costs and benefits are not symmetric and that high rates of HGT can act as a hedge against competitors with unpredictable T6SS efficacy. We conclude that antagonism and horizontal transfer drive successive rounds of weapon optimization and selective sweeps, dynamically shaping the composition of microbial communities.

IMPORTANCE The contact-dependent type VI secretion system (T6SS) is frequently used by *Proteobacteria* to kill adjacent competitors. While DNA released by T6 killing can be horizontally acquired, it remains untested whether T6 genes themselves can be horizontally acquired and then utilized to compete with neighboring cells. Using naturally transformable *Vibrio cholerae*, we provide the first direct empirical support for the hypothesis that T6 genes are exchanged horizontally (e.g., from dead competitors) and functionally deployed to compete with neighboring cells. Using computational simulations, we also demonstrate that high rates of HGT can be adaptive, allowing *V. cholerae* to improve upon existing T6 weaponry and survive direct encounters with otherwise superior competitors. We anticipate that our evolutionary results are of broad microbiological relevance, applying to many bacteria capable of HGT that utilize the T6SS or similar antagonistic systems, and highlight the profound impact of HGT in shaping microbial community structure.

KEYWORDS type VI secretion, *Vibrio cholerae*, genetics, horizontal gene transfer, natural transformation systems

Received 20 April 2017 **Accepted** 19 June 2017 **Published** 25 July 2017

Citation Thomas J, Watve SS, Ratcliff WC, Hammer BK. 2017. Horizontal gene transfer of functional type VI killing genes by natural transformation. mBio 8:e00654-17. https://doi.org/10.1128/mBio.00654-17.

Editor Bonnie Bassler, Princeton University

Address correspondence to Brian K. Hammer, brian.hammer@biology.gatech.edu.

* Present address: Samit S. Watve, Tufts University School of Medicine, Boston, Massachusetts, USA.

J.T. and S.S.W. contributed equally to this paper.

Horizontal gene transfer (HGT) by plasmid conjugation, viral transduction, and natural transformation plays a fundamental role in the evolution of bacteria and archaea and also in plants and other eukaryotes (1). Genomic analyses implicate HGT as a major factor responsible for the mosaic genomes of many bacteria, including the waterborne microbe *Vibrio cholerae*, which often carries the cholera toxin (CTX)-encoding prophage responsible for major cholera outbreaks in Haiti and regions of endemicity (2–5). *V. cholerae* isolates from aquatic environments are invariably non-

toxigenic (CTX$^-$) and commonly associated with chitinous surfaces like shells of crabs or zooplankton that may promote transmission (6).

All sequenced isolates of *V. cholerae* encode a type VI secretion system (T6SS) weapon that can deliver toxic effector proteins directly into grazing predators, diverse proteobacteria, and other *V. cholerae* bacteria that lack cognate immunity proteins (reviewed in references 7 to 11). The majority of nonclinical isolates express the T6SS constitutively, in the absence of chitin, likely as a competitive strategy in complex microbial communities of environmental biofilms (12, 13). In contrast, the majority of toxigenic clinical *V. cholerae* isolates engage in contact-dependent T6 killing only when triggered by the presence of chitin (14, 15), perhaps downregulating this activity in a host (9). Interestingly, chitin can also induce natural transformation in clinical isolates, which can promote HGT events due to lysis of adjacent nonimmune neighbors (14). Genome analyses of *V. cholerae* and other *Vibrio* species suggest that T6 loci encoding distinct effectors and adjacent cognate immunity factors, yet flanked by highly conserved sequence, may themselves be horizontally acquired by homologous recombination (16–18). Furthermore, it was hypothesized, but not experimentally tested, that HGT of distinct effector-immunity pairs could enable populations to diversify by generating individuals compatible with their competitor, yet susceptible to kin (16, 18). Whether HGT of novel T6 genes is adaptive in communities where kin and nonkin are in close proximity is unclear. Most clinical *V. cholerae* strains, which constitute the majority of sequenced and characterized isolates, carry identical T6 loci, thus hampering efforts to address this challenge.

We recently demonstrated that two sequenced *V. cholerae* strains with two syntenic T6 loci encoding distinct effector-immunity pairs behaved as "mutual killers" that precipitated a phase separation when cocultured (19). One strain is derived from clinical reference isolate C6706, which is induced by chitin to simultaneously express both the DNA uptake apparatus and the T6SS. The other is a recently sequenced environmental isolate 692-79 (20) which is defective at DNA uptake and yet is T6SS proficient. Here, we show that coculturing of these two strains in the presence of chitin induces unidirectional horizontal transfer of novel T6 effector-immunity pairs to the clinical isolate by homologous recombination. Transformants are simultaneously protected from attack by the environmental donor and susceptible to attack by former siblings. We modeled this process to gain insight into the evolutionary and ecological dynamics of T6-mediated competition. The fitness costs and benefits from acquisition and replacement of distinct T6SS effectors are contextual and should depend on the spatial structure of the population, the relative efficacy of T6SS effectors, and the rate of horizontal transfer. These results demonstrate that members of microbial communities can continuously adapt to diverse competitors by rapid acquisition of new molecular weaponry via horizontal transfer.

RESULTS

The core T6SS components of all sequenced *V. cholerae* strains are encoded in three operons—one main cluster and two auxiliary clusters, Aux1 and Aux2 (Fig. 1), while additional T6SS loci that may encode new effector-immunity pairs thought to be dispensable for assembly of the T6SS spike are occasionally present (18, 21). Each operon terminates in a gene encoding a toxic effector, immediately followed by its cognate immunity gene. In the toxigenic C6706 strain, the main cluster effector protein, VgrG-3, is a "specialized" effector that forms a physical component of the puncturing spike tip, while the Aux1 and Aux2 effectors are "cargo" effectors that each require a specific Tap (T6SS adaptor protein) or PAAR (proline-alanine-alanine-arginine) repeat domain protein as a chaperone for assembly with its cognate VgrG spike protein (8, 22). Aux1 and -2 operons of all sequenced *V. cholerae* strains have conserved DNA sequences flanking a variable region of differing percent GC content that encodes the effector-immunity pair, Tap, and C terminus of VgrG (18). The main T6SS cluster is entirely conserved between *V. cholerae* strains except for a short VgrG-3 C terminus and a portion of the immunity gene.

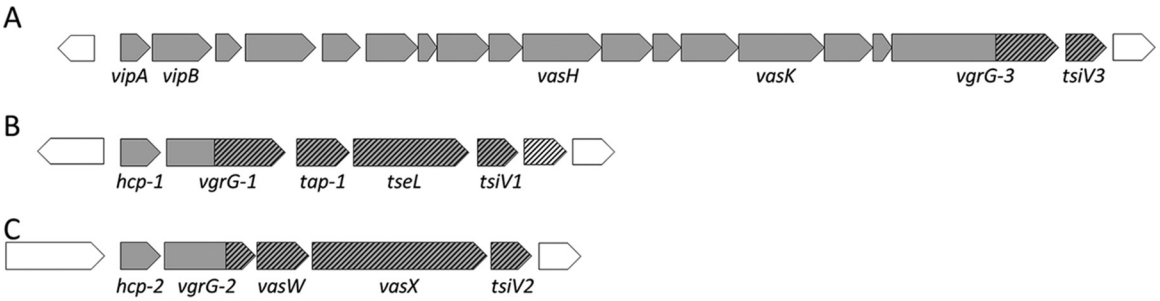

FIG 1 Organization of T6SS operons in *Vibrio cholerae* C6706. T6SS genes, shaded in gray, are organized into one large cluster (A) and two auxiliary clusters, Aux1 (B) and Aux2 (C). Hatched regions are variable compared to other sequenced *V. cholerae* isolates. The first gene of each of the auxiliary clusters encodes the major subunit of the protein tube, Hcp. Genes encoding effector and immunity proteins are *vgrG-3* and *tsiV3* (main cluster), *tseL* and *tsiV1* (Aux1), and *vasX* and *tsiV2* (Aux2), respectively.

As genomic analyses predict that transfer of entire T6SS operons frequently occurs in nature (16, 18), we tested this experimentally with toxigenic reference strain C6706, which is induced by chitin to become naturally transformable, and a nontransformable environmental isolate, 692-79 (12). At the Aux1 locus, both strains have distinct phospholipase effectors: TseL in C6706 and a phospholipase similar to Tle1 of *Pseudomonas aeruginosa* in 692-79 (23, 24). The Aux2 operons of the two strains encode effectors with entirely different activities: a VasX pore-forming protein in C6706 and a LysM domain-containing effector that potentially targets peptidoglycan in 692-79 (25, 26). We recently demonstrated that the distinct T6 activities of these strains allowed them to engage in mutually antagonistic T6S killing (19). We therefore predicted that horizontal transfer of T6SS genes via natural transformation from a 692-79 donor to a C6706 recipient would generate transformants with T6SS profiles distinct from both donor and recipient strains. To test whether we could observe C6706 transformants that acquired the Aux alleles of the 692-79 donor, we introduced antibiotic resistance cassettes by recombination directly downstream of the Aux1 or Aux2 immunity genes in the 692-79 strain. To avoid challenges interpreting exchange of core and regulatory components, we did not design a system to measure exchange of large cluster components. When the two strains were cocultured on chitin tiles submerged in artificial seawater (ASW), C6706 acquired the entire Aux1 or Aux2 operon of 692-79 by natural transformation at frequencies of ~1×10^{-6}, while a nontransformable C6706 mutant lacking the *comEA* gene did not (see Fig. S1 in the supplemental material). Acquisition of each T6SS operon was confirmed by PCR analysis. C6706 cultured with chitin was able to acquire both Aux1 and Aux2 T6SS alleles either from genomic DNA derived from 692-79 or by coculture with the donor strain (Fig. S1), and successive rounds of chitin-induced transformation also generated a C6706 transformant with both Aux1 as well as Aux2 allele replacements. Since acquisition by homologous recombination of a new T6SS operon is accompanied by a simultaneous loss of the original alleles, we initially expected that transformants would be selected against due to T6S killing by neighboring former clone mates. However, T6SS inactivation by deletion of *vasK* encoding an assembly protein (27) had modest effects on acquisition frequency of new T6SS operons either when using genomic donor DNA or in coculture (Fig. S1). We suspect that this is likely because the substrate-adherent cell-cell contact required for T6SS-mediated killing is not consistently maintained under the seawater conditions used in our transformation assays.

Recombination of each entire Aux cluster in the C6706 transformants was verified by sequencing the effector and immunity genes and a stretch of DNA 2 kb upstream of the start codon of the first gene in each operon. Sequencing confirmed acquisition of both the effector and immunity genes of the 692-79 donor, but newly acquired T6SS effectors must be expressed, properly folded, and loaded onto the T6SS complex encoded by the recipient strain if they are to be functional. Indeed, we found that the C6706 transformants with the Aux1 T6SS operon from 692-79 (which we refer to here

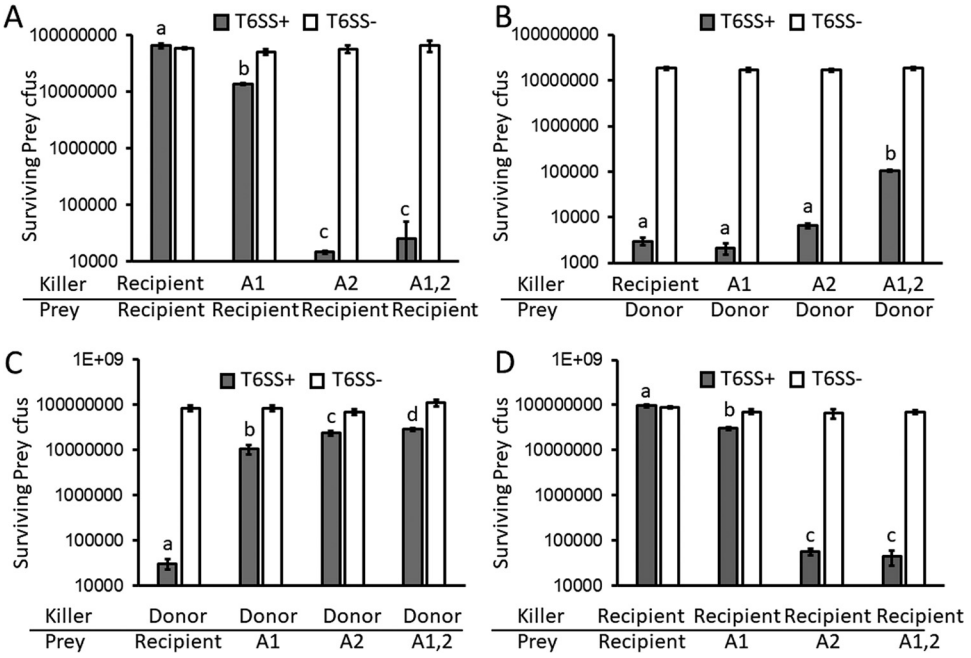

FIG 2 Horizontally acquired T6SS effectors and immunity proteins are functional in the recipient strain. "Killer" strains and T6SS$^-$ Δ*vasK* "prey" strains were mixed at a 10:1 ratio and incubated at 37°C for 3 h on membrane filters, and surviving prey CFU were counted on selective medium. Killer strains were either T6SS$^+$ (gray bars) or T6SS$^-$ (Δ*vasK*, white bars). Strains used were C6706 (recipient), 692-79 (donor), and C6706 derivatives in which either Aux1 (A1), Aux2 (A2), or both clusters (A1,2) were replaced by those of 692-79. Bars denote means ± standard deviations ($n = 4$ biological replicates, one representative experiment shown of two performed). T6SS$^+$ genotypes with different letters (a, b, c, d) exhibited mean survival different from those of other T6SS$^+$ genotypes ($P < 0.05$, ANOVA and Tukey's HSD) within the same experiment (panel).

as A1), the Aux2 operon (A2), and both operons (A1,2) are able to kill C6706 to an increasing degree in standard 3-h T6 killing assays ($F_{3,12} = 241.5$, $P < 0.0001$ [Fig. 2A]; differences in treatments for T6SS$^+$ experiments in Fig. 2 were assessed via analysis of variance [ANOVA] and Tukey's honestly significant difference [HSD]). Acquisition of either cluster also diminished the ability of transformants to kill 692-79; however, replacement of both clusters did not completely abrogate killing of 692-79 ($F_{3,12} = 983.2$, $P < 0.0001$ [Fig. 2B]). We predicted that the residual killing activity might be due to expression of the main cluster VgrG-3 of C6706, which was not replaced in these experiments. Indeed, deletion of *vgrG-3* in the double (A1,2) transformant completely abolished killing of the donor 692-79 (Fig. S2). Replacement of T6SS clusters also changed the immunity profiles of each strain: a single or double Aux cluster replacement protected the transformant from killing by the 692-79 donor ($F_{3,12} = 126.5$, $P < 0.0001$ [Fig. 2C]) but made the strains susceptible to killing by the C6706 recipient (parent), with the largest effect seen in the Aux1,2 transformant ($F_{3,12} = 446.5$, $P < 0.0001$ [Fig. 2D]).

A previous study demonstrated that the effector-immunity alleles carried by *Vibrio cholerae* V52 (and C6706) were the most potent in pairwise competition experiments among the different allele combinations tested (18). To examine the relative fitness of each T6SS transformant with respect to the recipient (parent) and donor, we performed pairwise 24-h competition experiments (Fig. 3). Acquisition of each T6SS cluster (with the exception of Aux1,2 versus Aux1) conferred a significant advantage to the transformant relative to the recipient (Fig. 3A). Statistical significance was established via two-tailed one-sample *t* tests with a Bonferroni correction for multiple comparisons. All tests with T6SS$^+$ genotypes were significant ($P < 0.01$, Fig. 3A and C), with the exception of Aux1,2 versus Aux1 (Fig. 3A), which had a postcorrection *P* value of 0.076. In every other case, transformants carrying an Aux1 (A1), Aux2 (A2), or both Aux1 and 2 (A1,2) replacement had increased fitness over both recipient and donor (Fig. 3A), with

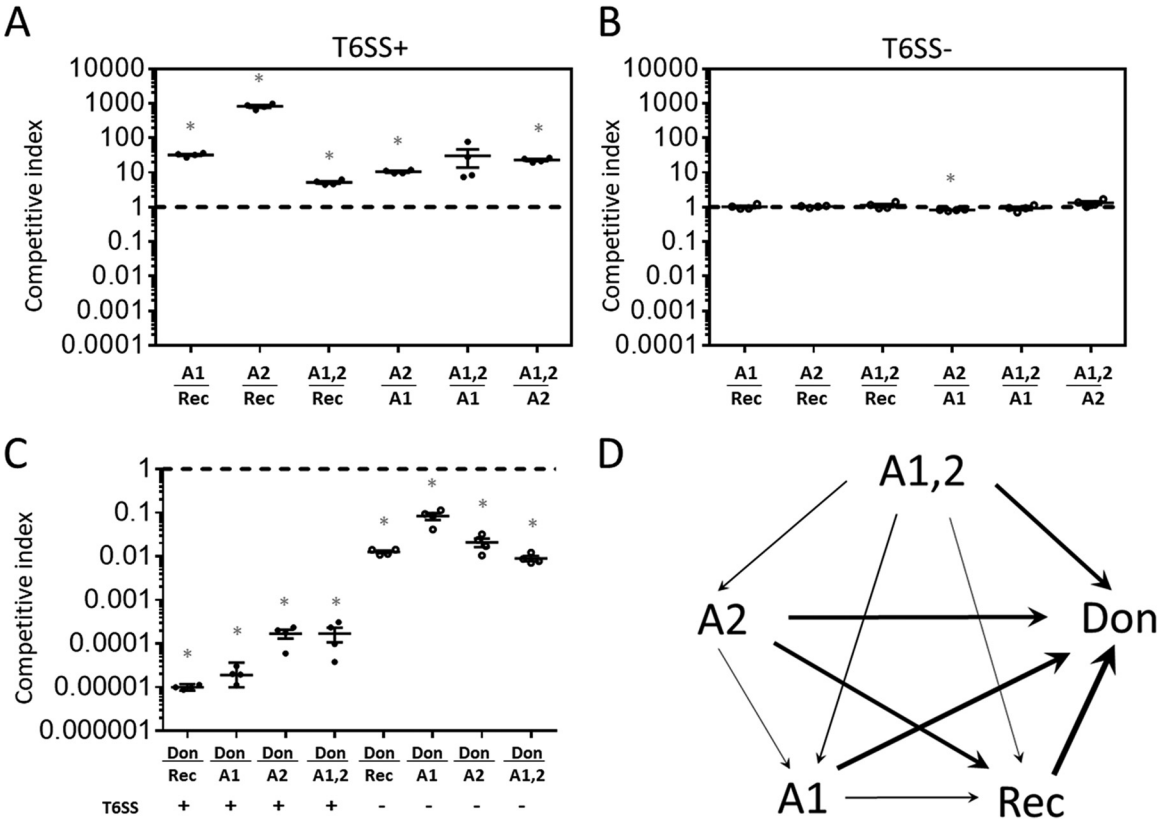

FIG 3 Acquisition of T6SS effectors from a donor (692-79) is beneficial to the recipient (C6706). (A to C) Pairwise competitions were set up between the recipient strain C6706 (Rec), the donor 692-79 (Don), and C6706 derivatives in which either Aux1 (A1), Aux2 (A2), or both clusters (A1,2) were replaced by those of 692-79. Strains were mixed at a 1:1 ratio and incubated on solid agar in a 12-well plate at 37°C for 24 h, and survivors of each strain were counted on selective medium. Both strains were T6SS$^+$ (A and C, closed circles) or T6SS$^-$ (Δ*vasK*, B and C, open circles). Competitive indices are measured as the final ratio of survivors divided by the initial ratio of inoculation. Horizontal lines in each cluster indicate geometric means of competitive indices. (D) The competitive hierarchy of strains analyzed in panels A to C is represented with arrows proceeding from the more fit competitor toward the less fit competitor. The line weight of each arrow is proportional to the $\log_{10}$ of the geometric mean of the competitive indices of the (more fit/less fit) competitor. Geometric mean and geometric standard deviation are represented for each cluster in panels A to C ($n = 4$ biological replicates, one representative experiment shown of two performed). Asterisks denote a competitive index significantly ($P < 0.05$) different from 1 (Bonferroni-corrected two-tailed one-sample *t* tests).

only marginal competitive differences observed in T6SS$^-$ controls (Fig. 3B). The A1,2 transformant has a competitive advantage over every other strain tested, suggesting that when 692-79 is the donor, acquisition of T6SS alleles by HGT is always beneficial to the C6706 recipient. However, the donor has a large T6SS-independent fitness defect compared to C6706 and its derivatives (Fig. 3C) and represents a potentially rare example of a poor competitor that carries superior weapons. To verify the competitive hierarchy that we observed in two-partner competitions (Fig. 3D), we cocultured C6706 and each transformant (A1, A2, and A1,2) in an initial 1:1:1:1 ratio for 5 days with back dilution and repeat passaging every 24 h (Fig. S3). We found that the A1,2 transformant dominated the mixed culture within 24 h and that the relative representation of the other strains was in agreement with the hierarchy observed in two-partner competitions (Fig. 3). Thus, HGT of T6SS allows C6706 to rapidly improve its repertoire of T6SS weaponry.

Our experimental results highlight a specific scenario of transfer of T6SS clusters. In order to derive general principles for how natural selection might act on the HGT of T6SS clusters, we extended a model that we previously developed to consider growth and competition on a two-dimensional lattice between any two mutually antagonistic strains (19). In our simulation, each strain possessed three distinct T6SS alleles. The "recipient" strain was capable of sequentially replacing its T6 effectors with those obtained from the "competitor" strain (see Materials and Methods for model details). As

in our experiments, the recipient was capable of HGT, but the donor was not. We observed that HGT can have a profound impact on T6SS-mediated competition dynamics. When the recipient possesses inferior T6SS effectors, HGT events precipitate a series of selective sweeps resulting in transformants that have completely replaced their T6SS alleles with those obtained from the superior competitor strain (Movie S1). As a result, HGT allows for competitive rescue of a strain that encodes an inferior set of T6SS alleles (relative T6SS efficiency, <1). More generally, the consequences of HGT on the fitness of the recipient genotype depend on how its T6SS loci compare to those of its competitor and the degree to which the population is spatially structured (Fig. 4A relative to 4B). Higher HGT rates are favored when a competitor possesses superior T6SS alleles but are costly when the competitor's T6SS alleles are inferior (Fig. 4). The benefits of HGT are far greater when the population is highly structured with each strain spatially separated (e.g., Fig. 4A), since T6 cluster replacement via HGT takes time. When the population is highly structured, the superior competitor takes more time to displace the recipient, which allows sufficient time for HGT and allelic replacement of T6SS clusters. The fitness valley in Fig. 4A occurs when horizontally acquired T6SS alleles are slightly better than those possessed by the recipient, allowing them to kill their clone mates, but not enough to escape their geometric disadvantage and spread. As a result, HGT drives high rates of intraclonal conflict, reducing their relative fitness.

T6SS-mediated conflict is inherently risky, as competitors vary widely in their relative killing efficacy (18). While HGT may allow a strain with inferior T6SS effectors to survive an interaction with a superior competitor in which it might otherwise be eradicated, HGT may also be costly, as rare transformants that acquire foreign T6SS loci immediately turn on adjacent former clone mates and are usually killed (Movie S1). While it is clear that incorporating inferior T6SS effectors will be costly, this is a separate cost from intrastrain genetic conflict, which occurs even when superior T6SS effectors are obtained horizontally. To estimate the fitness consequences of HGT-mediated intrastrain conflict, we simulated competition when mutually antagonistic recipients and competitors had distinct T6SS clusters that nonetheless killed with equal efficacy and then varied the HGT rate (Fig. 5, blue points). We measured the geometric mean fitness, as this best predicts long-term changes in the frequency of each T6 effector and is especially useful for taking variance in fitness across generations into account (28). Within-strain conflict, which can be estimated by the regression of fitness on HGT rate when partners do not vary (blue points; $y = -74.2x + 0.991$, $r^2 = 0.99$), was very costly, reducing fitness by 40% when the per-cell probability of HGT per time point was 0.005.

The fact that HGT incurs significant costs due to intrastrain conflict and benefits via survival when facing a superior competitor raises the possibility that it may act as a hedge against uncertainty in the T6SS efficacy of future opponents. We examined this hypothesis by calculating a recipient strain's geometric mean fitness across a pair of interactions in which it faced a competitor with symmetrically varying T6SS efficacy (there was thus no overall bias in favor of either strain) and across a range (0 to 0.005) of HGT. A geometric mean fitness above 1 indicates that HGT is adaptive. When the two strains have T6SSs with similar efficacies, the costs of HGT (intrastrain conflict) exceed its benefits and selection acts against HGT (Fig. 5). However, when competitor quality is highly variable, HGT can be adaptive, with selection favoring very high rates of transformation (Fig. 5). The valley-shaped distribution of fitness for the high-variance treatments is a consequence of the geometry of competition: when HGT rates are low, transformants are surrounded by former clone mates that can now kill them via T6SS. Isolated transformants have a low probably of surviving killing attempts by their neighbors, even if they have moderately superior T6SS alleles. Higher rates of HGT lead to rare but important multiple transformation events where two or more adjacent cells take up a competitor's allele, reducing their geometric disadvantage and dramatically increasing the probability that they will precipitate a selective sweep. Note that even when HGT equals 0, variation in competitor T6SS increases the

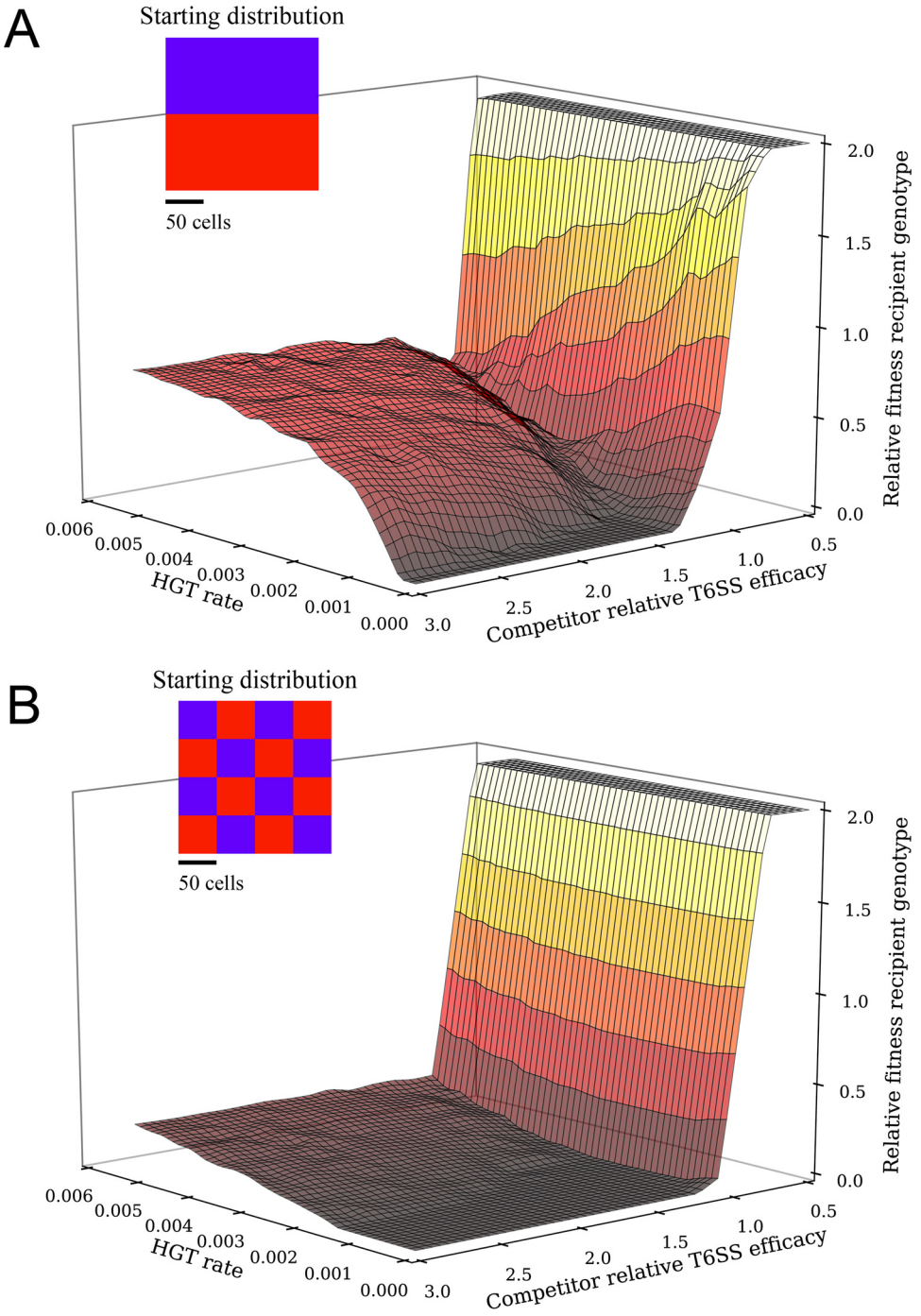

FIG 4 Costs and benefits of horizontally acquiring a competitor's T6SS. In this model of competition between two bacterial strains, one (the "recipient") was capable of integrating T6SS alleles from the other (the "competitor"). High rates of HGT were adaptive only when the recipient strain faced a competitor with superior T6SS alleles. For plotting purposes, relative fitness of >2 was clipped. Simulations were run for 15,000 time steps. Time-lapse videos of these fitness landscapes are shown in Movies S2 and S3.

recipient's fitness (Fig. 5). This reflects the cost of variability on the competitor's fitness (or, inversely, the relative benefit that the recipient experiences by not varying), a well-known phenomenon in evolutionary ecology (28). Thus, high rates of HGT were strongly beneficial when the competitor's T6SS efficacy was more variable, as the increased survival in the face of a superior competitor more than made up for HGT's costs.

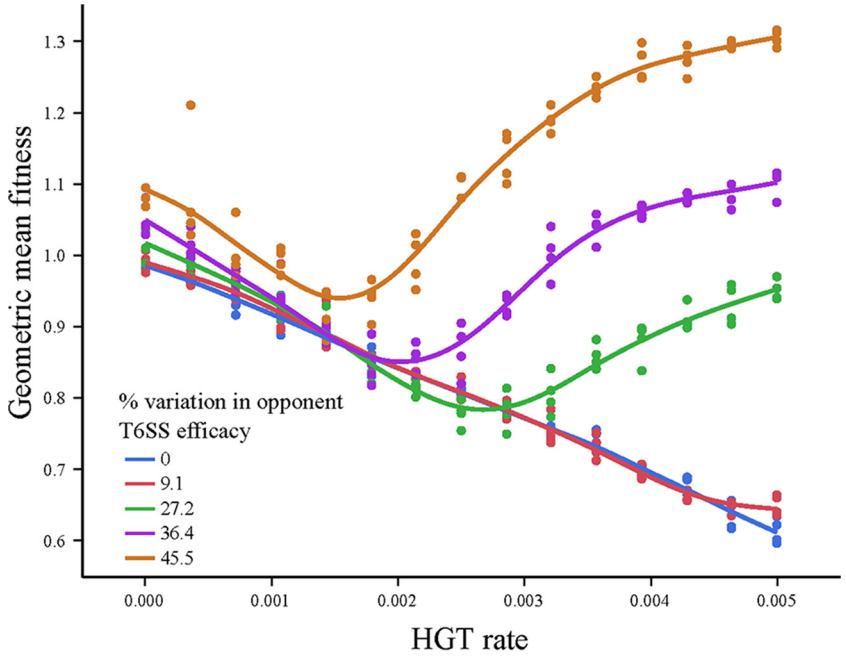

FIG 5 Horizontal gene transfer serves as a hedge against unpredictable competitors. To examine effects of variability in competitor T6SS efficacy on selection on HGT rate, the geometric mean fitness of the recipient genotype was determined across pairs of simulations, in which recipients faced competitors with increasingly high variation in T6SS efficacy (±0, 9.1, 27.2, 36.4, and 45.5% from its own T6SS).

DISCUSSION

We have demonstrated that toxigenic bacteria can acquire T6SS effector-immunity pairs from nontoxigenic neighbors via natural transformation, consistent with the hypothesis that this frequently occurs in the environment (16, 18). Once acquired, the novel T6SS effector-immunity proteins are functional and can contribute toward T6SS-mediated antagonism against neighboring cells as well as provide immunity against T6SS attacks by neighbors. Interestingly, transformants that undergo successive HGT of T6SS effector-immunity pairs have increased fitness relative to either parental strain in direct competition experiments, reaffirming the fundamental role of HGT in shaping bacterial ecology and evolution. To provide ecological and evolutionary context for these results, we used an agent-based model to explore how HGT of T6SS could affect spatial patterning in surface-attached populations and generate hypotheses for how key parameters (i.e., population spatial structure, rate of HGT, relative efficacy of T6SS alleles between competitor strains, and variance in competitor T6SS efficacy) might affect bacterial fitness. Our modeling reveals that HGT can be quite costly: a cell runs the risk of incorporating an inferior T6SS allele, and every transformant must overcome the geometric disadvantage of being surrounded by former clone mates to which it is no longer fully immune. Still, these costs are more than compensated for when an HGT$^+$ strain is facing a competitor with far superior T6SS alleles. Indeed, we show that variability in opponent T6SS allele quality alone can select for high rates of HGT, allowing HGT to act as a hedge against uncertain opponent quality.

In our experimental system, we were only able to observe examples of T6SS cluster replacement. However, bioinformatic and phylogenetic approaches have recently identified lineages of *V. cholerae* that appear to have undergone multiple rounds of additive HGT at a single highly recombinogenic T6SS locus to form "immunity gene arrays" encoding several putative T6SS immunity proteins, which may provide protection against effectors from multiple *V. cholerae* and non-*V. cholerae* strains (16). Successive acquisition of the immunity genes likely benefits the transforming lineage in three ways. First, a recipient strain gains immunity against a diverse set of T6SS$^+$ competitors. Second, the recipient avoids the metabolic cost of expressing nonnative effectors.

Third, retention of the existing effector-immunity pair (as opposed to the replacement observed here) avoids costs of intrastrain genetic conflict. Thus, additive recombination represents an additional mechanism to promote horizontal spread of T6SS alleles while mitigating the costs of HGT.

In toxicogenic *V. cholerae* strains C6706 and A1552, both natural transformation and T6S are coinduced under conditions of chitin utilization, starvation, and quorum sensing at high cell density (14, 15). Specifically, activation of the quorum sensing system by *Vibrio*-specific autoinducer molecules induces the DNA uptake machinery (29, 30). This concordance suggests that *V. cholerae* may have evolved to acquire genes, including T6S effector-immunity pairs, from recently killed competitors. This has, until now, presented a conundrum: why acquire genes from defeated, inferior competitors? While it is unclear whether the bulk of horizontal transfer events occur during active T6-mediated competition, our work demonstrates that the acquisition of novel T6SSs can provide an efficient route to means-test novel weaponry, which may be strongly favored by natural selection if competitor T6S efficacy varies widely through time. More generally, our results suggest that the interplay of antagonism and horizontal transfer results in successive rounds of combat, arms trading, and selective sweeps that may dynamically shape diverse microbial communities.

MATERIALS AND METHODS

Bacterial strains and culture conditions. All *V. cholerae* strains were derivatives of El Tor C6706 *str-2* (31) or environmental strain 692-79 (see Table S1 in the supplemental material). Bacteria were routinely grown at 37°C in lysogeny broth (LB) under constant shaking or statically on LB agar, supplemented with ampicillin (100 μg/ml), kanamycin (50 μg/ml), chloramphenicol (10 μg/ml for *V. cholerae* and 25 μg/ml for *Escherichia coli*), spectinomycin (100 μg/ml), streptomycin (5 mg/ml), and diaminopimelic acid (50 μg/ml) where appropriate.

Recombinant DNA techniques and construction of *V. cholerae* mutants. In-frame deletions and promoter-replacement mutants in *V. cholerae* were constructed by previously described allelic exchange methods (32). Standard molecular biology-based methods were utilized for DNA manipulations. DNA-modifying enzymes and restriction nucleases (Promega and New England Biolabs); Gibson assembly mix (New England Biolabs); and Q5, Phusion, and OneTaq DNA polymerases (New England Biolabs) were used according to the manufacturer's instructions. All recombinant DNA constructs were tested by PCR and verified by Sanger sequencing (Eurofins).

Transformation assays. Assays for natural transformation were performed as previously described (33). Briefly, the recipient strain was back diluted from an overnight liquid culture and grown at 37°C in LB with shaking until it reached an optical density at 600 nm (OD_{600}) of 0.4 to 0.6. Cultures were washed in artificial seawater (ASW) and diluted to an OD_{600} of 0.15, and 2-ml cultures in ASW were incubated at 30°C with a chitin tile for 24 h. The chitin tile with adherent bacteria was moved to 2 ml fresh ASW containing 1 μg/ml of genomic DNA marked with an antibiotic resistance cassette and incubated at 30°C for a further 24 h. Cells were collected by washing the chitin tile in 2 ml of fresh ASW, and dilutions were plated on selective medium to determine transformation frequency. Acquisition of T6SS alleles from donor DNA linked to the antibiotic resistance cassette was verified by allele-specific multiplex PCR using primers specific for C6706 or 697-79. Transformation in coculture was performed as described above with the following exceptions: both donor and recipient strain were each grown to an OD_{600} of 0.4 to 0.6 in LB and diluted to an OD_{600} of 0.15 after washing in ASW mixed in a 1:1 ratio, and 2 ml of each mixed culture was inoculated with a chitin tile at 30°C. No exogenous genomic DNA was added.

Killing assays. T6SS killing assays were performed as previously described (15). Killer and prey strains grown overnight in LB at 37°C were centrifuged and resuspended in fresh medium to an OD_{600} of 1.00. Killer and prey strains were mixed at a ratio of 10:1, and 50 μl of each suspension was spotted onto a gridded filter disc (Whatman) placed on an LB agar plate and confined to 9 grid squares (3.1 by 3.1 mm each) to reduce variability. Filters were incubated at 37°C for 3 h and washed with 5 ml LB to dislodge cells, and dilutions were plated on selective medium to determine prey survival.

Pairwise competitions. Competitor strains were grown overnight in LB at 37°C, centrifuged, and resuspended in fresh medium to an OD_{600} of 1.00. Pairs of strains were mixed 1:1, and 50 μl of each suspension was inoculated on LB agar plugs in a 12-well plate, dried under laminar airflow in a biosafety cabinet, and incubated overnight at 37°C. Cells were resuspended in 1 ml LB, and dilutions were plated on selective medium to determine survival of each competitor. Competitive index was determined as final ratio of survivors/initial ratio of inoculation.

Statistical analysis. All statistics were calculated in JMP 12.0. T6SS efficacy (Fig. 2A to D) was calculated by ANOVA, followed by Tukey's honestly significant difference (HSD) *post hoc* test, with an α of 0.05. Within each experiment (i.e., figure panel), different letters denote significantly different means. The consequence of horizontal acquisition of T6SS effectors for pairwise interactions (Fig. 3) was examined by two-tailed one-sample *t* tests (i.e., testing the null hypothesis that the competitive index is 1) with a Bonferroni correction to control for multiple comparisons. Competitive indices were $\log_{10}$ transformed prior to analysis to give equal weight to competitive ratios both above and below 1.

Individual-based simulation. We extended the individual-based model from the work of McNally et al. (19). Square lattices (200 × 200) were seeded with an equal number of "recipient" and "competitor" genotype cells. Biologically, this is analogous to a population growing across a solid surface, such as a crab shell. The starting conditions for Fig. 4 are shown as insets; all other simulations use the well-separated population shown in Fig. 4A. At each time point, 5% of the cells in the population were selected to reproduce if an adjacent space was unoccupied. Similarly, 5% of the cells in the population were selected to activate their T6SS. The probability that they killed a neighboring cell depended on the difference between their T6SS effector-immunity pairs and the relative killing efficiency of those effectors. The three effectors possessed by each genotype were assumed to act in an additive manner, and so the probability of killing was determined by summing across the number of effector-immunity pairs that differed between the strains, weighted by the efficacy of those effector alleles. For example, a matchup in which the recipient is inferior might be the following: the recipient genotype has three effectors, each of which confers an 0.11 probability of killing a susceptible competitor genotype cell, while the competitor has three different effectors, each of which offers an 0.33 probability of killing a susceptible recipient genotype cell. A recipient genotype cell would therefore have a 33% chance of killing an adjacent competitor cell, while the competitor would have a 100% chance of killing an adjacent recipient cell.

Recipient genotype cells had a probability, ranging from 0 to 0.005, of replacing one of their T6SS effector protein-immunity pair alleles with one obtained from the environment at each time step. This was performed in a weighted manner, according to the frequency of recipient versus competitor alleles in the population, and did not depend on the spatial distribution of those cells in the population. Biologically, this is analogous to cells sampling DNA from a well-mixed bulk medium above a surface-attached population. Note that this means that HGT can occur in both directions, with the recipient genotype replacing its T6SS with those from the competitor and, in future HGT events, reverting to its original T6SS genotype. HGT events occur in a stepwise manner, and so only one allele can be replaced per time point. The probability that adjacent cells succeed in killing was calculated as the sum of the per-allele killing probability for all of the T6SS loci that differ between the cells. Simulations were run in Python (code available upon request). Edges (outermost rows/columns) were trimmed prior to analysis. For Fig. 4 and Movies S2 and S3, fitnesses were calculated as the ratio of recipient to genotype cells at time point *t*, divided by their starting ratio. The fitness landscapes shown in these figures were calculated across a 20-by-20 factorial combination of HGT rates and competitor T6SS efficacies for 15,000 time points.

Assessing fitness with variable competitors. We examined whether or not HGT could act as a hedge against unpredictable competitors by simulating pairs of interactions, in which the T6SS killing efficacy of the recipient strain varied symmetrically (i.e., ±9.1, 27.2, 36.4, or 45.5% above and below) around the competitor's killing efficacy. We calculated the geometric mean of fitness (raw fitness calculated as described above) for these pairs of interactions across a range of HGT rates (0 to 0.005), with five replicates of the simulation run per treatment combination.

SUPPLEMENTAL MATERIAL

Supplemental material for this article may be found at https://doi.org/10.1128/mBio.00654-17.

FIG S1, TIF file, 0.1 MB.
FIG S2, TIF file, 0.1 MB.
FIG S3, TIF file, 0.1 MB.
TABLE S1, DOCX file, 0.01 MB.
MOVIE S1, AVI file, 7.8 MB.
MOVIE S2, MOV file, 9.9 MB.
MOVIE S3, MOV file, 8.4 MB.

ACKNOWLEDGMENTS

We thank members of the Hammer lab for helpful discussions regarding this paper.

This work was supported by the Gordon and Betty Moore Foundation grant number 4308.07 and NSF grant number MCB-1149925 to B.K.H. and NSF grant number DEB-1456652, NASA Exobiology grant number NNX15AR33G, and a Packard Foundation Fellowship to W.C.R. The funders had no role in study design, data collection and interpretation, or the decision to submit the work for publication.

Author contributions were as follows: J.T. and S.S.W., conception and design, acquisition of data, analysis and interpretation of data, and drafting or revising the article; W.C.R., conception and design, acquisition of data, analysis and interpretation of data, drafting or revising the article, and funding acquisition; and B.K.H., conception and design, analysis and interpretation of data, drafting or revising the article, funding acquisition, and project administration.

REFERENCES

1. Soucy SM, Huang J, Gogarten JP. 2015. Horizontal gene transfer: building the web of life. Nat Rev Genet 16:472–482. https://doi.org/10.1038/nrg3962.
2. Chun J, Grim CJ, Hasan NA, Lee JH, Choi SY, Haley BJ, Taviani E, Jeon YS, Kim DW, Lee JH, Brettin TS, Bruce DC, Challacombe JF, Detter JC, Han CS, Munk AC, Chertkov O, Meincke L, Saunders E, Walters RA, Huq A, Nair GB, Colwell RR. 2009. Comparative genomics reveals mechanism for short-term and long-term clonal transitions in pandemic *Vibrio cholerae*. Proc Natl Acad Sci U S A 106:15442–15447. https://doi.org/10.1073/pnas.0907787106.
3. Katz LS, Petkau A, Beaulaurier J, Tyler S, Antonova ES, Turnsek MA, Guo Y, Wang S, Paxinos EE, Orata F, Gladney LM, Stroika S, Folster JP, Rowe L, Freeman MM, Knox N, Frace M, Boncy J, Graham M, Hammer BK, Boucher Y, Bashir A, Hanage WP, Van Domselaar G, Tarr CL. 2013. Evolutionary dynamics of *Vibrio cholerae* O1 following a single-source introduction to Haiti. mBio 4:e00398-13. https://doi.org/10.1128/mBio.00398-13.
4. Meibom KL, Blokesch M, Dolganov NA, Wu CY, Schoolnik GK. 2005. Chitin induces natural competence in *Vibrio cholerae*. Science 310:1824–1827. https://doi.org/10.1126/science.1120096.
5. Waldor MK, Mekalanos JJ. 1996. Lysogenic conversion by a filamentous phage encoding cholera toxin. Science 272:1910–1914. https://doi.org/10.1126/science.272.5270.1910.
6. Pruzzo C, Vezzulli L, Colwell RR. 2008. Global impact of *Vibrio cholerae* interactions with chitin. Environ Microbiol 10:1400–1410. https://doi.org/10.1111/j.1462-2920.2007.01559.x.
7. Alcoforado Diniz J, Liu YC, Coulthurst SJ. 2015. Molecular weaponry: diverse effectors delivered by the type VI secretion system. Cell Microbiol 17:1742–1751. https://doi.org/10.1111/cmi.12532.
8. Durand E, Cambillau C, Cascales E, Journet L. 2014. VgrG, Tae, Tle, and beyond: the versatile arsenal of type VI secretion effectors. Trends Microbiol 22:498–507. https://doi.org/10.1016/j.tim.2014.06.004.
9. Joshi A, Kostiuk B, Rogers A, Teschler J, Pukatzki S, Yildiz FH. 2017. Rules of engagement: the type VI secretion system in *Vibrio cholerae*. Trends Microbiol 25:267–279. https://doi.org/10.1016/j.tim.2016.12.003.
10. Russell AB, Peterson SB, Mougous JD. 2014. Type VI secretion system effectors: poisons with a purpose. Nat Rev Microbiol 12:137–148. https://doi.org/10.1038/nrmicro3185.
11. Cianfanelli FR, Monlezun L, Coulthurst SJ. 2016. Aim, load, fire: the type VI secretion system, a bacterial nanoweapon. Trends Microbiol 24:51–62. https://doi.org/10.1016/j.tim.2015.10.005.
12. Bernardy EE, Turnsek MA, Wilson SK, Tarr CL, Hammer BK. 2016. Diversity of clinical and environmental isolates of *Vibrio cholerae* in natural transformation and contact-dependent bacterial killing indicative of type VI secretion system activity. Appl Environ Microbiol 82:2833–2842. https://doi.org/10.1128/AEM.00351-16.
13. Ishikawa T, Sabharwal D, Bröms J, Milton DL, Sjöstedt A, Uhlin BE, Wai SN. 2012. Pathoadaptive conditional regulation of the type VI secretion system in *Vibrio cholerae* O1 strains. Infect Immun 80:575–584. https://doi.org/10.1128/IAI.05510-11.
14. Borgeaud S, Metzger LC, Scrignari T, Blokesch M. 2015. The type VI secretion system of *Vibrio cholerae* fosters horizontal gene transfer. Science 347:63–67. https://doi.org/10.1126/science.1260064.
15. Watve SS, Thomas J, Hammer BK. 2015. CytR is a global positive regulator of competence, type VI secretion, and chitinases in *Vibrio cholerae*. PLoS One 10:e0138834. https://doi.org/10.1371/journal.pone.0138834.
16. Kirchberger PC, Unterweger D, Provenzano D, Pukatzki S, Boucher Y. 2017. Sequential displacement of type VI secretion system effector genes leads to evolution of diverse immunity gene arrays in *Vibrio cholerae*. Sci Rep 7:45133. https://doi.org/10.1038/srep45133.
17. Salomon D, Klimko JA, Trudgian DC, Kinch LN, Grishin NV, Mirzaei H, Orth K. 2015. Type VI secretion system toxins horizontally shared between marine bacteria. PLoS Pathog 11:e1005128. https://doi.org/10.1371/journal.ppat.1005128.
18. Unterweger D, Miyata ST, Bachmann V, Brooks TM, Mullins T, Kostiuk B, Provenzano D, Pukatzki S. 2014. The *Vibrio cholerae* type VI secretion system employs diverse effector modules for intraspecific competition. Nat Commun 5:3549. https://doi.org/10.1038/ncomms4549.
19. McNally L, Bernardy E, Thomas J, Kalziqi A, Pentz J, Brown SP, Hammer BK, Yunker PJ, Ratcliff WC. 2017. Killing by type VI secretion drives genetic phase separation and correlates with increased cooperation. Nat Commun 8:14371. https://doi.org/10.1038/ncomms14371.
20. Watve SS, Chande AT, Rishishwar L, Mariño-Ramírez L, Jordan IK, Hammer BK. 2016. Whole-genome sequences of 26 *Vibrio cholerae* isolates. Genome Announc 4:e01396-16. https://doi.org/10.1128/genomeA.01396-16.
21. Altindis E, Dong T, Catalano C, Mekalanos J. 2015. Secretome analysis of *Vibrio cholerae* type VI secretion system reveals a new effector-immunity pair. mBio 6:e00075-15. https://doi.org/10.1128/mBio.00075-15.
22. Unterweger D, Kostiuk B, Pukatzki S. 2017. Adaptor proteins of type VI secretion system effectors. Trends Microbiol 25:8–10. https://doi.org/10.1016/j.tim.2016.10.003.
23. Dong TG, Ho BT, Yoder-Himes DR, Mekalanos JJ. 2013. Identification of T6SS-dependent effector and immunity proteins by Tn-seq in *Vibrio cholerae*. Proc Natl Acad Sci U S A 110:2623–2628. https://doi.org/10.1073/pnas.1222783110.
24. Russell AB, LeRoux M, Hathazi K, Agnello DM, Ishikawa T, Wiggins PA, Wai SN, Mougous JD. 2013. Diverse type VI secretion phospholipases are functionally plastic antibacterial effectors. Nature 496:508–512. https://doi.org/10.1038/nature12074.
25. Brooks TM, Unterweger D, Bachmann V, Kostiuk B, Pukatzki S. 2013. Lytic activity of the *Vibrio cholerae* type VI secretion toxin VgrG-3 is inhibited by the antitoxin TsaB. J Biol Chem 288:7618–7625. https://doi.org/10.1074/jbc.M112.436725.
26. Miyata ST, Kitaoka M, Brooks TM, McAuley SB, Pukatzki S. 2011. *Vibrio cholerae* requires the type VI secretion system virulence factor VasX to kill *Dictyostelium discoideum*. Infect Immun 79:2941–2949. https://doi.org/10.1128/IAI.01266-10.
27. Ma LS, Lin JS, Lai EM. 2009. An IcmF family protein, ImpLM, is an integral inner membrane protein interacting with ImpKL, and its Walker A motif is required for type VI secretion system-mediated Hcp secretion in *Agrobacterium tumefaciens*. J Bacteriol 191:4316–4329. https://doi.org/10.1128/JB.00029-09.
28. Simons AM. 2009. Fluctuating natural selection accounts for the evolution of diversification bet hedging. Proc Biol Sci 276:1987–1992. https://doi.org/10.1098/rspb.2008.1920.
29. Antonova ES, Hammer BK. 2011. Quorum-sensing autoinducer molecules produced by members of a multispecies biofilm promote horizontal gene transfer to *Vibrio cholerae*. FEMS Microbiol Lett 322:68–76. https://doi.org/10.1111/j.1574-6968.2011.02328.x.
30. Suckow G, Seitz P, Blokesch M. 2011. Quorum sensing contributes to natural transformation of *Vibrio cholerae* in a species-specific manner. J Bacteriol 193:4914–4924. https://doi.org/10.1128/JB.05396-11.
31. Thelin KH, Taylor RK. 1996. Toxin-coregulated pilus, but not mannose-sensitive hemagglutinin, is required for colonization by *Vibrio cholerae* O1 El Tor biotype and O139 strains. Infect Immun 64:2853–2856.
32. Skorupski K, Taylor RK. 1996. Positive selection vectors for allelic exchange. Gene 169:47–52. https://doi.org/10.1016/0378-1119(95)00793-8.
33. Watve SS, Bernardy EE, Hammer BK. 2014. Vibrio cholerae: measuring natural transformation frequency. Curr Protoc Microbiol 35:6A.4.1–6A.412. https://doi.org/10.1002/9780471729259.mc06a04s35.